Accurate finite elements based on shear deformation theory for the analysis of laminated composite plates

V.E. Verijenko[1] and S. Adali[2] and E.B. Summers[3]

(First received July 1992; Final version May 1993)

Abstract

A finite element formulation for the analysis of laminated composite plates based on a higher-order theory is presented. This formulation leads into a discrete-continuous scheme where the surface of the laminate is discretized with each finite element forming a heterogeneous continuum through the thickness. Rectangular and triangular finite elements are formulated. The degrees of freedom of the nodal points of these elements are independent of the number of layers. Nonlinear laws governing the variation of the components of the displacement vector and of the stress and strain tensors through the thickness of layers are taken into account. The laminate may also exhibit heterogeneous properties in the plane of the plate, where elements with different properties are used as an approximation. The elements are applied to the bending of laminated plates with various loading and boundary conditions and numerical results are obtained. The solutions presented are compared with those obtained using the three-dimensional elasticity theory, and with the closed form solutions of other authors. It is shown that the present approach reduces the number of unknown variables and broadens the field of application of the finite element method.

Nomenclature

u_i, w	Displacement
$\epsilon_{ij}, \kappa_{ij}$	Deformation of the reference surface
e_{ij}	Components of the strain tensor
σ_{ij}	Components of the stress tensor
χ	Shear function
φ_k	Distribution functions for shear deformation
ψ_k	Distribution functions for tangential displacement
E	Modulus of elasticity
G	Shear modulus
ν	Poisson's ratio
Q	Shear forces
M	Bending moments
D	Stiffness characteristics
η, ξ	Dimensionless coordinates
K	Stiffness matrix
$v, \bar{v}$	Degrees of freedom of the nodal points
R	Vector of nodal forces

1 Introduction

Fibre-reinforced composites are now widely used in many engineering applications for their exceptional strength and stiffness properties relative to their weight. Therefore it is important to be able to accurately model the behaviour of structural components such as plates manufactured from these advanced materials. It is well known that the use of classical plate theory, which is based on the Kirchoff assumptions, leads to intolerable errors in the analysis of composite structures. If the phenomenon of transverse shear is neglected, even the deflection of thin laminated plates are underpredicted when the laminae differ significantly in their elastic properties.

Numerous approaches have been suggested which take into account the three-dimensional stress and strain behaviour of multilayered plates based on two-dimensional higher-order theories. Details of different higher-order theories and their finite element modelling may be found in reviews [1–5]. However, as mentioned in [6] and in the review [2], some of the theories exhibit no compatibility between the nonlinear kinematic model, which considers the distortion of the normal, and the system of internal forces and moments equivalent to those obtained using the 'straight line' hypothesis.

A higher-order theory of laminated plates and shells without these drawbacks has been formulated by the authors and is presented in [7–9]. This theory considers plates with transversely isotropic layers of different thicknesses, stiffnesses, and densities, in which the number and sequence of layers are arbitrary. The physical and mechanical characteristics of each layer are variable through the thickness and the layers are assumed to be perfectly bonded. The equations for the tangential components of the displacement vector and the stress and strain tensors consist of similar terms which separately take into account the states of pure bending and transverse shear. This important feature enables the efficient numerical application of this theory using an independent but analogous approximation of the components of the displacement vector.

[1] Associate Professor, Department of Mechanical Engineering, University of Natal, King George V Avenue, Durban, 4001 Republic of South Africa

[2] Professor of Solid Mechanics

[3] PhD candidate

2 Rectangular element of laminated plate

In this section, a rectangular element with transversely isotropic layers of different thicknesses, which takes into account shear deformation, is formulated. The basic equations are expressed for a model which includes transverse shear under the normal loading p_3. Since there is no shear load on the external surfaces of the plate, the tangential displacements of the reference surface are assumed to be negligible. The plate has dimensions of $a \times b$ and a total thickness of $a_0 + a_n$ as shown in Figure 1a. The reference surface is positioned such that the maximum transverse shear occurs at this surface.[9] These assumptions are acceptable in many practical engineering applications.[10]

In the following analysis a subscript after a comma denotes differentiation with respect to the variable following the comma, and k refers to the k-th layer. The displacements of the plate in the x_1, x_2 and z directions are denoted by u_1, u_2 and w, respectively.

The basic equations for the shear-deformable model are

$$\begin{aligned} u_i^{(k)} &= w_{,i} z - \chi_{,i} \psi_k; \\ i &= 1,2; \\ w(x_i) &\approx u_3^{(k)}(x_i, z); \\ e_{ij}^{(k)} &= \kappa_{ij}^{(1)} \psi_k; \\ 2e_{i3}^{(k)} &= \chi_{,i} \varphi_k; \\ e_{33}^{(k)} &= 0; \\ j &= 1,2 \end{aligned} \tag{1}$$

where $\kappa_{ij} = -w_{,ij}, \kappa_{ij}^{(1)} = -\chi_{,ij}$, and χ is a new unknown function which is called the 'shear function'.[11] The graphical interpretation of this kinematic model is given in Figure 2. The distribution functions of the tangential displacements ψ_k and shear deformations φ_k through the thickness of layers are expressed as

$$\begin{aligned} \varphi_k(z) &= f_{1k}/G'_k; \\ \psi_k(z) &= \int_0^z (\varphi_{1k} - \varphi_k) dz \end{aligned} \tag{2}$$

where

$$\begin{aligned} \varphi_{1k}(z) &= \int_0^z \nu'_{0k} z dz; \\ \nu'_{0k} &= E_k \nu'_k / E'_k (1 - \nu_k); \\ f_{1k}(z) &= f_k^* - f_k B_1 B^{-1}; \\ f_k(z) &= \int_{a_0}^z E_{0k} dz; \\ f_k^*(z) &= \int_{a_0}^z E_{0k} z dz; \\ E_{0k} &= E_k / (1 - \nu_k^2); \\ B &= \int_{a_0}^{a_n} G_{0k} dz; \\ B_1 &= \int_{a_0}^{a_n} G_{0k} \psi_k dz; \\ G_{0k} &= 2G_k / (1 - \nu_k) \end{aligned} \tag{3}$$

where $E_k(z)$, $\nu_k(z)$ and $G_k(z) = E_k/[2(1+\nu_k)]$ are the modulus of elasticity, Poisson's ratio and shear modulus, respectively, in the plane of isotropy and $E'_k(z)$, $G'_k(z)$, $\nu'_k(z)$ are these characteristics in transverse direction.

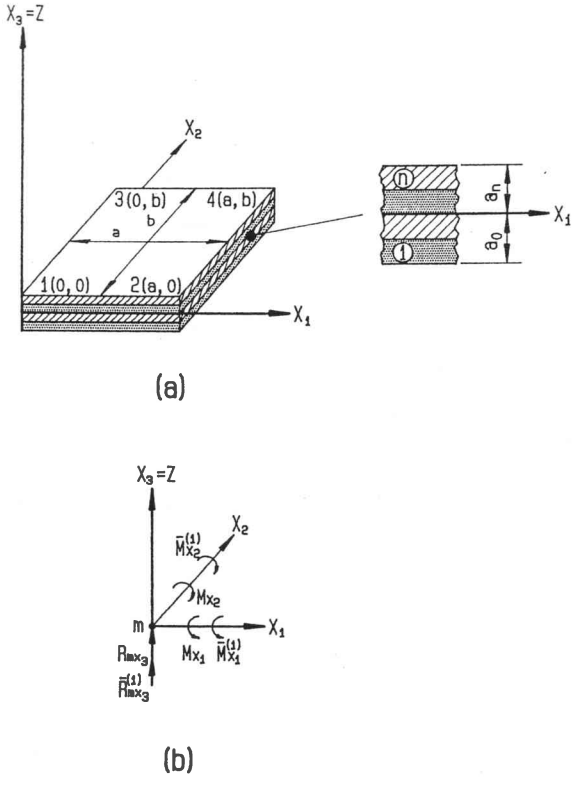

Figure 1. Rectangular finite element, (a) general view, (b) nodal reactions.

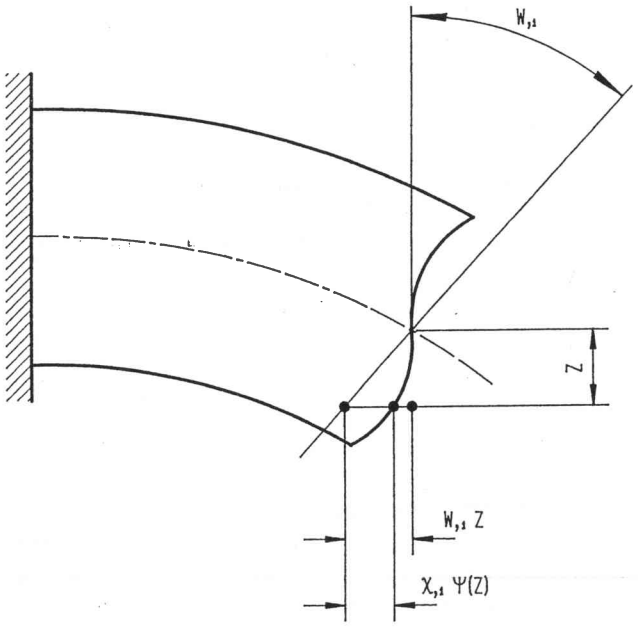

Figure 2. Kinematic model for shear-deformable theory.

The corresponding static model is given by

$$\begin{aligned}
\sigma_{33}^{(k)} &= 0 \\
\sigma_{11}^{(k)} &= G_{0k}\left[(\kappa_{11}+\nu_k\kappa_{22})\,z+\left(\kappa_{11}^{(1)}+\nu_k\kappa_{22}^{(1)}\right)\right]\psi_k \\
\sigma_{22}^{(k)} &= \sigma_{11}^{(k)} \\
\sigma_{12}^{(k)} &= G_{0k}\,(1-\nu_k)\left[\kappa_{12}z+\kappa_{12}^{(1)}\psi_k\right] \\
\sigma_{i3} &= \chi_{,i}f_{1k}
\end{aligned} \tag{4}$$

The variation of potential energy of the r-th element now may be expressed as

$$\delta\Pi_r = \int\int_{S_r}\left[-M_{ij}\delta w_{,ij}-\bar{M}_{ij}^{(1)}\delta\bar{w}_{,ij}^{(1)}+\bar{Q}_i^{(1)}\delta\bar{w}_{,i}^{(1)}\right]dS_r \tag{5}$$

where the generalized displacement $\bar{w}^{(1)} = D_{00}^{-1}D_{01}\chi$, S_r is the r-th element. The forces $\bar{Q}_i^{(1)}$ and the moments $\bar{M}_{ij}$, $\bar{M}^{(1)}$ are defined as

$$\begin{aligned}
\bar{Q}_i^{(1)} &= D_{00}D_{01}^{-1}Q_i^{(1)} = D_{00}D_{01}^{-1}\textstyle\int_{a_0}^{a_n}\sigma_{i3}^{(k)}\psi_{k,z}dz \\
M_{ij} &= \textstyle\int_{a_0}^{a_n}\sigma_{ij}^{(k)}zdz \\
\bar{M}_{ij}^{(1)} &= D_{00}D_{01}^{-1}M_{ij}^{(1)} = D_{00}D_{01}^{-1}\textstyle\int_{a_0}^{a_n}\sigma_{ij}^{(k)}\psi_k dz
\end{aligned} \tag{6}$$

where the following stiffness characteristics [10] are required

$$\begin{aligned}
D_{00} &= \textstyle\int_{a_0}^{a_n}G_{0k}z^2dz \\
D_{01} &= \textstyle\int_{a_0}^{a_n}G_{0k}\psi_k z dz
\end{aligned} \tag{7}$$

The variation of the external load is

$$\delta H_r = \int\int_{S_r} p_3\delta w dS_r \tag{8}$$

The derivation of the rectangular finite element is now given for multilayered plates. Six degrees of freedom are assigned to each nodal point (see Figure 1b). The first three degrees of freedom correspond to the deformation caused by the bending and are the deflection w and the two angles of rotation α and β about the axes x_1, x_2 ($\alpha = w_{,2}$; $\beta = -w_{,1}$). The remaining three degrees of freedom correspond to the shear deformation $\bar{w} = \bar{w}^{(1)}$ which is analogous to deflection and to $\bar{\alpha} = \varphi_2^{(1)}$, $\bar{\beta} = -\varphi_1^{(1)}$ which are analogous to angles of rotation. Thus at each nodal point $m = 1,2,3,4$ of the element r in the local coordinate system, two groups of displacements are defined by

$$\begin{aligned}
\{v_m\} &= \{w_m,\alpha_m,\beta_m\}^T; \\
\{\bar{v}_m\} &= \{\bar{w}_m,\alpha_m,\beta_m\}^T
\end{aligned} \tag{9}$$

which relate to the deformation of the reference surface.

The approximation of the displacement in the region of the FE may be introduced in the well-known form [12]

$$\begin{aligned}
w(x) &= a_1+a_2x_1+a_3x_2+a_4x_1^2+a_5x_1x_2 \\
&\quad +a_6x_2^2+a_7x_1^3+a_8x_1^2x_2+a_9x_2^2 \\
&\quad +a_{10}x_2^3+a_{11}x_1^3x_2+a_{12}x_1x_2^3 \\
\bar{w}(x) &= \bar{a}_1+\bar{a}_2x_1+\bar{a}_3x_2+\bar{a}_4x_1^2+\bar{a}_5x_1x_2 \\
&\quad +\bar{a}_6x_2^2+\bar{a}_7x_1^3+\bar{a}_8x_1^2x_2+\bar{a}_9x_1x_2^2 \\
&\quad +\bar{a}_{10}x_2^3+\bar{a}_{11}x_1^3+\bar{a}_{12}x_1x_2^3
\end{aligned} \tag{10}$$

which may be written as

$$\begin{aligned}
w(x) &= \sum_{m=1}^{4}\left(w_m\Theta_{m1}+\alpha_m\Theta_{m2}+\beta_m\Theta_{m3}\right) \\
\bar{w}(x) &= \sum_{m=1}^{4}\left(\bar{w}_m\Theta_{m1}+\bar{\alpha}_m\Theta_{m2}+\bar{\beta}_m\Theta_{m3}\right)
\end{aligned} \tag{11}$$

where the system of approximation functions

$\{\Theta_{mt}(x),\ m = 1,\ ...,\ 4;\ t = 1,2,3\}$

are given by

$$\begin{aligned}
\Theta_{11}(\xi,\eta) &= 1-3\xi^2-\xi\eta-3\eta^2+2\xi^3+3\xi^2\eta \\
&\quad +3\xi\eta^2+2\eta^3-2\xi^3\eta-2\xi\eta^3 \\
\Theta_{12}(\xi,\eta) &= b\left(\eta-\xi\eta-2\eta^2+2\xi\eta^2+\eta^3-\xi\eta^3\right) \\
\Theta_{13}(\xi,\eta) &= a\left(-\xi+\xi\eta+2\xi^2-2\xi^2\eta-\xi^3+\xi^3\eta\right) \\
\Theta_{21}(\xi,\eta) &= 3\xi^2+\xi\eta-2\xi^3-3\xi\eta^2+2\xi^3\eta \\
&\quad +2\xi\eta^3-3\xi^2\eta \\
\Theta_{22}(\xi,\eta) &= b\left(\xi\eta-2\xi\eta^2+\xi\eta^3\right) \\
\Theta_{23}(\xi,\eta) &= a\left(\xi^2-\xi^3-\xi^2\eta+\xi^3\eta\right) \\
\Theta_{31}(\xi,\eta) &= 3\eta^2+\xi\eta-2\eta^3-3\xi\eta^2-3\xi^2\eta \\
&\quad +2\xi\eta^3+2\xi^3\eta \\
\Theta_{32}(\xi,\eta) &= b\left(-\eta^2+\eta^3+\xi\eta^2-\xi\eta^3\right) \\
\Theta_{33}(\xi,\eta) &= a\left(-\xi\eta+2\xi^2\eta-\xi^3\eta\right) \\
\Theta_{41}(\xi,\eta) &= -\xi\eta-3\xi^2\eta+3\xi\eta^2-2\xi^3\eta-2\xi\eta^3 \\
\Theta_{42}(\xi,\eta) &= b\left(-\xi\eta^2+\xi\eta^3\right) \\
\Theta_{43}(\xi,\eta) &= a\left(\xi^2\eta-\xi^3\eta\right)
\end{aligned} \tag{12}$$

where $\xi = x_1a^{-1}$ and $\eta = x_2b^{-1}$ are dimensionless coordinates.

The stiffness matrix for element r may be obtained from equations (5) using (12), and may be expressed as

$$[K]_r = [K_{gs}]_r = \begin{bmatrix} K_{11} & K_{12} \\ K_{21} & K_{22} \end{bmatrix}; \quad g,s = 1,2 \tag{13}$$

where each block is symmetric. The submatrix K_{11} corresponds to the state of bending and is identical to the stiffness matrix for a homogeneous plate [12]. The submatrix K_{22} corresponds to the state of transverse shear, and the submatrices K_{12}, K_{21} characterize the interaction of these states. The dimensions of the submatrices in (13) are 12×12, and therefore the dimension of the matrix (13)

Table 1 Stiffness matrix for rectangular elements

Reactions		Degrees of freedom											
		1	2	3	4	5	6	7	8	9	10	11	12
		w_1	α_1	β_1	w_2	α_2	β_2	w_3	α_3	β_3	w_4	α_4	β_4
1	R_{1x_3}	k_{11}	k_{12}	k_{13}	k_{14}	k_{15}	k_{16}	k_{17}	k_{18}	k_{19}	k_{110}	k_{111}	k_{112}
2	M_{1x_1}		k_{22}	k_{23}	k_{24}	k_{25}	k_{26}	k_{27}	k_{28}	k_{29}	k_{210}	k_{211}	k_{212}
3	M_{1x_2}			k_{33}	k_{34}	k_{35}	k_{36}	k_{37}	k_{38}	k_{39}	k_{310}	k_{311}	k_{312}
4	R_{2x_3}				k_{44}	k_{45}	k_{46}	k_{47}	k_{48}	k_{49}	k_{410}	k_{411}	k_{412}
5	M_{2x_1}					k_{55}	k_{56}	k_{57}	k_{58}	k_{59}	k_{510}	k_{511}	k_{512}
6	M_{2x_2}						k_{66}	k_{67}	k_{68}	k_{69}	k_{610}	k_{611}	k_{612}
7	R_{3x_3}							k_{77}	k_{78}	k_{79}	k_{710}	k_{711}	k_{712}
8	M_{3x_1}								k_{88}	k_{89}	k_{810}	k_{811}	k_{812}
9	M_{3x_2}		Symmetric							k_{99}	k_{910}	k_{911}	k_{912}
10	R_{4x_3}										k_{1010}	k_{1011}	k_{1012}
11	M_{4x_1}											k_{1111}	k_{1112}
12	M_{4x_2}												k_{1212}

is 24×24. The entries of the submatrix K_{11} are given in Table 1 and Appendix A. The submatrix K_{12} is similar to K_{11} where the entries $k_{l(t+12)}(l,t=1,...,12)$ are equal to the corresponding entries of K_{11} when $\nu_{11}=\bar{D}_{00}/D_{00}$ is replaced with $\nu_{12}=\bar{D}_{01}D_{01}^{-1}$. In this case the following stiffnesses are required

$$\begin{aligned}
\bar{D}_{00} &= D_{00}-\tfrac{B_1^2}{B}\\
\bar{D}_{01} &= \int_{a_0}^{a_n} A_{12k}\psi_k z dz\\
A_{12k} &= \Delta_{12k}/\Delta_k\\
\Delta_k &= (1+\nu_k)\left[1-\nu_k-2\left(\nu_k'\right)^2 E_k/E_k'\right]/E_k^2E_k'\\
\Delta_{12k} &= \left[\nu_k+\left(\nu_k'\right)^2 E_k/E_k'\right]/E_kE_k'
\end{aligned} \tag{14}$$

The entries of the submatrix K_{22} can be determined in terms of the entries k_{lt} as

$$k_{(l+12)(t+12)}=\left(c_{22}k_{lt}+c_2\alpha_{lt}\right)c_{21}^{-1} \tag{15}$$

where

$$c_{22}=D_{11}D_{10}^{-1}\quad c_{21}=D_{10}D_{00}^{-1}\quad c_2=D_1D_{10}^{-1}$$

and α_{lt} are additional quantities used in the calculation of the coefficients of shear (see Appendix B). It is noted that ν_{11} has been replaced with $\nu_{22}=\bar{D}_{11}D_{11}^{-1}$ in the coefficients k_{lt} of stiffness matrix, where

$$\begin{aligned}
D_{11} &= \int_{a_0}^{a_n} G_{0k}\psi_k^2 dz;\\
D_1 &= D_{10}=D_{01};\\
\bar{D}_{11} &= D_{11}-\tfrac{B_1^2}{B}
\end{aligned} \tag{16}$$

If the load $p_3=q$ is uniform over the finite element, then the vector of nodal forces of the element r is given by

$$\{R\}_r=\frac{qab}{24}\{6,b,-a,6,b,a,6,-b,-a,6,-b,a\}_r^T \tag{17}$$

In the case of a point load applied in the centre of the rectangular element, the vector of equivalent forces is given by

$$\{R\}_r=\frac{P}{16}\{4,b,-a,4,b,a,4,-b,-a,4,-b,a\}_r^T \tag{18}$$

As seen in equation (8), the load p_3 produces work over the displacements w. Therefore the components of the vector of nodal forces corresponding to the displacements $\bar{w}$ equal zero.

It is noted that the above element may also model the external loads by moments at the nodal points, and this improves the accuracy of the analysis.

The theory governing the finite elements requires two groups of constraints at the boundary of the plate. The first group, referred to as the 'external' boundary conditions, constrains the two-dimensional reference surface of plate and models the general type of support for the plate. The second group, referred to as the 'internal' boundary conditions, models the transverse deformations through the thickness at the boundary of the plate. These boundary conditions are modelled in terms of the degrees of freedom. Table 2 gives the details of the boundary conditions and the corresponding constraints.

3 Triangular element of laminated plate

This case differs only in the geometry of the finite element (see Figure 3a). At each nodal point m $(m=1,2,3)$ the group of displacements may be expressed as

$$\begin{aligned}
\{v_m\} &= \{w_m,\alpha_m,\beta_m\}^T\\
\{\bar{v}_m\} &= \{\bar{w}_m,\bar{\alpha}_m,\bar{\beta}_m\}^T
\end{aligned} \tag{19}$$

A fourth order polynomial is used to approximate the continuous displacement field.

The dimensionless coordinates

$$\xi=a^{-1}\left(x_1-c^{-1}bx_2\right);\quad \eta=c^{-1}x_2 \tag{20}$$

Table 2 Boundary conditions

External Conditions			
Hinged, Moving	Clamped	Clamped, Moving	Free End
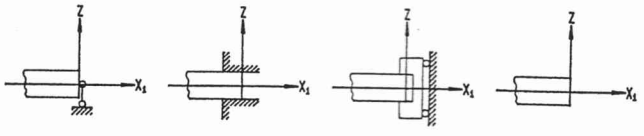			
Constraints			
$w = \alpha = 0$ $\beta \neq 0$	$w = \alpha = 0$ $\beta = 0$	$w \neq 0$ $\alpha = \beta = 0$	$w \neq 0$ $\alpha \neq 0 \neq \beta$

Internal Conditions			
Flexible out of the plane of the edge	Rigid	Flexible in the plane of the edge	No constraints (Free Edge)
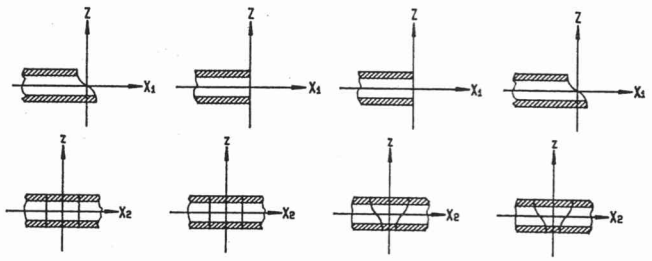			
Constraints			
$\bar{w} = \bar{\alpha} = 0$ $\bar{\beta} \neq 0$	$\bar{w} = \bar{\alpha} = 0$ $\bar{\beta} = 0$	$\bar{w} = \bar{\beta} = 0$ $\bar{\alpha} \neq 0$	$\bar{w} \neq 0$ $\bar{\alpha} \neq 0 \neq \bar{\beta}$

are introduced in order to simplify the formulation of the stiffness matrix (see Figure 3b).

In the new ξ, η coordinate system the vectors of the degrees of freedom of the nodal point m are given by

$$\begin{aligned} \{v_m\} &= \{w_m, \alpha_m^*, \beta_m^*\}^T \\ \{\bar{v}_m\} &= \{\bar{w}_m, \bar{\alpha}_m^*, \bar{\beta}_m^*\}^T \end{aligned} \tag{21}$$

where $\alpha_m^* = w_{m,\eta}$, $\beta_m^* = -w_{m,\xi}$, $\bar{\alpha}_m^* = \bar{w}_{m,\eta}$, and $\bar{\beta}_m^* = -\bar{w}_{m,\xi}$.

For each of these vectors there are nine approximation functions given by

$$\{\varphi_{mt}(\xi,\eta),\ m,\ t = 1,2,3\} \tag{22}$$

These functions may be expressed in explicit form as

$$\begin{aligned}
\varphi_{11}(\xi,\eta) &= 1 - 3\xi^2 - 3\eta^2 + 2\xi^3 + 2\eta^3 \\
&\quad +6(1-\lambda_1-\lambda_2)\Phi_1(\xi,\eta) + 12(\lambda_2 - 1) \\
&\quad \times\Phi_2(\xi,\eta) + 12(\lambda_1 - 1)\Phi_3(\xi,\eta) \\
\varphi_{12}(\xi,\eta) &= \eta(1-\eta)^2 - \xi^2\eta + (1 - 3\lambda_2)\Phi_1(\xi,\eta) \\
&\quad + (6\lambda_2 - 4)\Phi_2(\xi,\eta) - 2\Phi_3(\xi,\eta) \\
\varphi_{13}(\xi,\eta) &= \xi(1-\xi)^2 + \xi\eta^2 + (3\lambda_1 - 1)\Phi_1(\xi,\eta) \\
&\quad +2\Phi_2(\xi,\eta) + (4 - 6\lambda_2)\Phi_3(\xi,\eta) \\
\varphi_{21}(\xi,\eta) &= 3\xi^2 - 2\xi^3 + 12(1-\lambda_3)\Phi_2(\xi,\eta) + \\
&\quad (1-\lambda_1-\lambda_3)[12\Phi_3(\xi,\eta) - 6\Phi_1(\xi,\eta)] \\
\varphi_{22}(\xi,\eta) &= \xi^2\eta + (3\lambda_3 - 1)\Phi_1(\xi,\eta) + (4 - 6\lambda_3) \\
&\quad \times\Phi_2(\xi,\eta) + (2 - 6\lambda_3)\Phi_3(\xi,\eta) \\
\varphi_{23}(\xi,\eta) &= \xi^2 - \xi^3 + 6(1-\lambda_3)\Phi_2(\xi,\eta) + \\
&\quad (1-\lambda_1-\lambda_3)[6\Phi_3(\xi,\eta) - 3\Phi_1(\xi,\eta)] \\
\varphi_{31}(\xi,\eta) &= 3\eta^2 - 2\eta^3 + 12\lambda_3\Phi_3(\xi,\eta) + \\
&\quad (\lambda_2 - \lambda_3)[6\Phi_1(\xi,\eta) - 12\Phi_2(\xi,\eta)] \\
\varphi_{32}(\xi,\eta) &= -\eta^2 + \eta^3 + (\lambda_3 - \lambda_2)[3\Phi_1(\xi,\eta) \\
&\quad -6\Phi_2(\xi,\eta)] - 6\lambda_3\Phi_3(\xi,\eta) \\
\varphi_{33}(\xi,\eta) &= -\eta^2\xi + (3\lambda_3 - 2)\Phi_1(\xi,\eta) + (4 - 6\lambda_3) \\
&\quad \times\Phi_2(\xi,\eta) + (2 - 6\lambda_3)\Phi_3(\xi,\eta)
\end{aligned} \tag{23}$$

where

$$\begin{aligned}
\lambda_1 &= b/a; \\
\lambda_2 &= ab/(a^2 + c^2); \\
\lambda_3 &= (a-b)\,a/\left[c^2 + (a-b)^2\right]; \\
\Phi_1 &= \xi\eta - \xi^2\eta - \xi\eta^2; \\
\Phi_2 &= \xi^2\eta(1 - \xi - \eta); \\
\Phi_3 &= \xi\eta^2(1 - \xi - \eta)
\end{aligned} \tag{24}$$

The system of approximation functions

$$\{\Theta_{mt}(x_1, x_2);\quad m,t = 1,2,3\}$$

which are compatible with the degrees of freedom

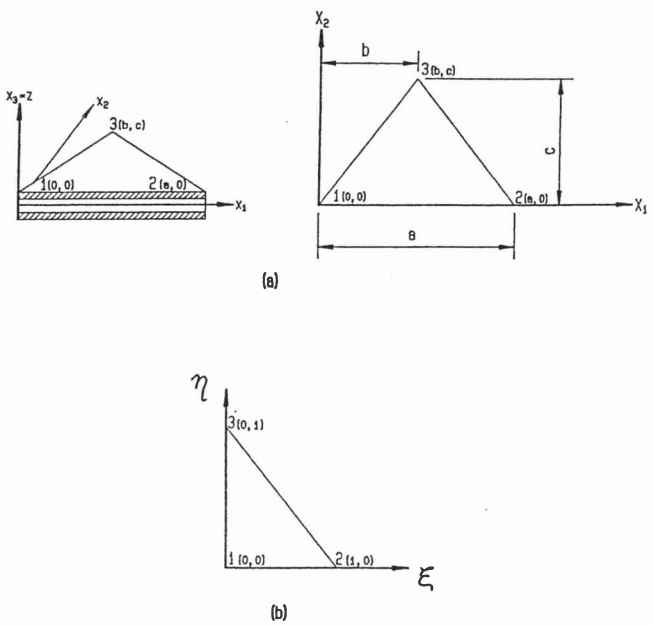

Figure 3. Triangular finite element, (a) general view, (b) dimensionless coordinate system.

w_m, α_m, β_m, $\bar{w}_m$, $\bar{\alpha}_m$, $\bar{\beta}_m$ in the $x_1 - x_2$ coordinate system are given as

$$\begin{aligned} \Theta_{m1}(x_1, x_2) &= \varphi_{m1}(\xi, \eta) \\ \Theta_{m2}(x_1, x_2) &= c\varphi_{m2}(\xi, \eta) \\ \Theta_{m3}(x_1, x_2) &= a\varphi_{m3}(\xi, \eta) - b\varphi_{m2}(\xi, \eta) \end{aligned} \tag{25}$$

Then the displacements in the finite element region may be written as

$$\begin{aligned} w &= \sum_{m=1}^{3} (w_m\Theta_{m1} + \alpha_m\Theta_{m2} + \beta_m\Theta_{m3}) \\ \bar{w} &= \sum_{m=1}^{3} (\bar{w}_m\Theta_{m1} + \bar{\alpha}_m\Theta_{m2} + \bar{\beta}_m\Theta_{m3}) \end{aligned} \tag{26}$$

Using equations (5), (23), and (24), the stiffness matrix of a triangular element of a laminated plate may be obtained explicitly. This matrix may also be represented in block form as given in equation (13).

4 Numerical results and discussion

The accuracy of the finite elements developed in sections 2 and 3 is now illustrated by means of numerical examples.

Example 1. As a first example, a three-layered square plate is considered with the dimensions $2a \times 2a$ and under a uniform load $p_3 = q = 10^5 \mathrm{Nm}^{-2}$. The 'external' boundary conditions are taken as simply supported and the 'internal' boundary conditions are taken as flexible out of plane of the edge, but rigid in this plane. The properties of the external (bearing) layers 1 and 3 are $h_1 = h_3 = 1 \times 10^{-3}$m, $E_1 = E_3 = 6.8 \times 10^4$ MPa, $G_1 = G_3 = 26\,150$MPa, and $\nu_1 = \nu_3 = 0.3$.

The properties of the filler layer $k = 2$ are $h_2 = 15 \times 10^{-3}$ m, $E_2 = 4\,800$ MPa, $G_2 = 380$ MPa, and $\nu_2 = 0.3$. The plate is divided into four rectangular finite elements. Noting the symmetry, the constraints of the nodal displacements may be expressed as

$$\begin{aligned} &x_1 = 0, x_2 = 0; \quad w_1 = \alpha_1 = \beta_1 = \bar{w}_1 = \bar{\alpha}_1 = \bar{\beta}_1 = 0 \\ &x_1 = a, x_2 = 0; \quad w_2 = \beta_2 = \bar{w}_2 = \bar{\beta}_2 = 0, \alpha_2 \neq 0, \bar{\alpha}_2 \neq 0 \\ &x_1 = 0, x_2 = a; \quad w_3 = \alpha_3 = \bar{w}_3 = \bar{\alpha}_3 = 0, \beta_3 \neq 0, \bar{\beta}_3 \neq 0 \\ &x_1 = a, x_2 = a; \quad \alpha_4 = \beta_4 = \bar{\alpha}_4 = \bar{\beta}_4 = 0, w_4 \neq 0, \bar{w}_4 \neq 0 \end{aligned} \tag{27}$$

The general vector of the nodal displacements is

$$\{V\} = \{v, \bar{v}\}^T = \{\alpha_2, \beta_3, w_4, \bar{\alpha}_2, \bar{\beta}_3, \bar{w}_4\}^T \tag{28}$$

Taking into account equation (17), the general vector of corresponding nodal forces is expressed as

$$\{R\}_r = \{R, \bar{R}\}^T = \{11.05\mathrm{Nm}, -11.05\mathrm{Nm}, 479\mathrm{N}, 0, 0, 0\}^T \tag{29}$$

The entries of the stiffness matrix $[K]$ may be determined using Table 1, Appendix A, Appendix B, and equation (14) where $D_{00} = 11.06$Nm, $c_{21} = 17.44 \times 10^{-1}\mathrm{m}^2$, $c_{22} = 17.48 \times 10^{-4}\mathrm{m}^2$, and $\nu_{11} = \nu_{12} = \nu_{22} = \nu = 0.3$. The system of algebraic equations may be written as

$$\begin{aligned} K_{11}v + K_{12}\bar{v} &= R \\ K_{21}v + K_{22}\bar{v} &= 0 \end{aligned} \tag{30}$$

Using the block principle [8] the solution is divided into two simpler systems

$$v = \left(K_{11} - \frac{K_{12}^2}{K_{22}}\right)^{-1} R; \quad \bar{v} = -\frac{K_{12}}{K_{22}}\left(K_{11} - \frac{K_{12}^2}{K_{22}}\right)^{-1} R \tag{31}$$

The solution gives the deflection at the centre of the plate as $w_4 = 3.56 \times 10^{-3}$m. The analytical solution for this case gives $w_{\max} = 3.05 \times 10^{-3}$m. When the number of finite elements along each side equals 4, 6, and 8, the corresponding maximum deflections of the plate are obtained as $w_{\max} = (3.19, 3.11, 3.08)\ 10^{-3}$m, respectively. The solution using Reissner's theory gives $w_{\max} = 3.16 \times 10^{-3}$m whereas the classical theory gives $w_{\max} = 2.16 \times 10^{-3}$m which is obviously inaccurate.

Example 2. Consider the bending of a square simply supported homogeneous plate of dimensions $a \times a$ subjected to sinusoidal loading $q\sin(\pi x_1/a)\sin(\pi x_2/a)$. The finite element results are compared with the exact solution given in [13]. The application of the finite elements developed in the previous sections produced accurate results even for a plate with a thickness ratio of $h/a = 1/5$. In this case the number of unknown is 3.5 times less than that of the case where 3-D elements are used (Table 3). Table 3 also gives the results for a three-layered symmetrical plate subjected to a sinusoidal loading. The thickness of the bearing layers is taken as $h_1 = h_3 = h/6$ and the thickness of the filler layer as $h_2 = (4/6)\,h$. The layers are isotropic with the elastic properties $E_1 = E_3 = 10^3 E_2$, $\nu_1 = \nu_2 = 0.3$. The boundary conditions are the same as in the first example. The thickness ratio h/a equals 1/10 . The discrete-continuous scheme (DCS) solution is compared with the analytical solution [14] and the 3-D finite element solution. Accurate results are obtained with the number of unknowns being approximately 10 times less than that of the case of 3-D elements as indicated in Table 3.

Table 3 Comparison of various solutions (Example 2)

Type of plate	Type of solution	$\tilde{w}$	$\tilde{\sigma}$	FE mesh	No. of unknown values
Homo-	Exact [12]	2.098	5.244		
geneous	FEM 3-D	1.96	5.42	$8 \times 8 \times 8$	336
$h/a = \frac{1}{5}$	FEM DCS	2.18	5.26	8×8	96
Three-	3-D [13]	925.9	125.1		
layered	FEM 3-D	904	118	$10 \times 10 \times 6$	1244
$h/a = \frac{1}{10}$	FEM DCS	914	125	10×10	150

where $\tilde{w} = w_{\max} E_1 (10qh)^{-1}$ and $\tilde{\sigma} = \sigma_{\max} q^{-1}$

Example 3. Consider a three-layered square plate supported at each of the four corners with the following characteristics: dimensions $a = 25h = 1$ m; total thickness of the laminate $h = 40 \times 10^{-3}$ m where the thickness of the

bearing layers is $h_1 = h_3 = 2 \times 10^{-3}$ m, and the thickness of the filler layer is $h_2 = 36 \times 10^{-3}$ m; elastic moduli $E_1 = E_3 = 7 \times 10^4$ MPa, $E_2 = 70$ MPa; Poisson's ratios $\nu_1 = \nu_2 = \nu_3 = 0.3$.

The maximum deflections and stresses in the bearing layers are given in Table 4 for the various types of 'internal' boundary conditions and loading (see Table 2). The types of internal boundary conditions listed are: (1) rigid in and out of the plane of the edge; (2) flexible out of the plane of the edge but rigid in the plane; (3) flexible in the plane but rigid out of the plane; (4) rigid at the corners with no constraints along the sides; and (5) no internal constraints.

The results for the deflections indicate three different types of boundary behaviour: firstly, for the first and second type of constraints, when the shear in the plane of the edges vanishes and the deflections are almost identical; secondly, for the third and fourth type of constraints, shear is allowed in the plane of the edge and the deflections increase by a factor of 1.5 to 2.2 in comparison with the first case for point and uniform loads; and thirdly, when there are no internal constraints to resist the shear, the deflections increase by a factor of 1.7 to 2.8 in comparison with the first case for the same type of loading. The results obtained for normal stresses at the centre of the plate indicate that the type of internal constraints have only a minor influence on these stresses in comparison with the type of support. The stresses on the edge depend more on the internal constraints than do the stresses away from the edge, and are 1.2 times greater for the cases 3–5 than those for the case 1.

Example 4. Consider the analysis of the plate in Example 1 using triangular elements. Results are given for various numbers of elements in Table 5, where the deflection is given in the form $\tilde{w} = 10^{-4} w_{\max} E_1 / q_3 h_1$ and the stresses in the external layers are given in the form $\tilde{\sigma} = \sigma_{\max}/q_3$. Deflections are also determined from the analytical solutions of various theories. Reissner's theory gives $\tilde{w} = 21.39$; the classical theory gives $\tilde{w} = 14.66$. Table 5 shows that the triangular elements give accurate results.

Table 5 Convergency of results for triangular elements (Example 4)

Number of elements	Elements based on Shear-deformable theory $\tilde{w}$	$\tilde{\sigma}$
4	17.25	167
16	19.70	176
64	20.47	205
256	20.65	213

5 Summary and conclusions

The finite element formulation presented above leads to a discrete-continuous scheme for the analysis of laminated composite plates where each finite element forms a heterogeneous continuum through the thickness. On the basis of this scheme, rectangular and triangular finite elements are developed which take into account the deformation of

Table 4 Solution for a 3-layered plate (Example 3)

Loading	Type of internal boundary conditions	Deflections and stresses at the centre of the plate $\tilde{w}$	$\tilde{\sigma}$	Stresses at the edge $\tilde{\sigma}$
Sinusoidal $q \sin \frac{\pi x_1}{a} \sin \frac{\pi x_2}{a}$	1	27.35	916.3	873.3
	2	27.66	916.3	991.6
	3	53.52	916.7	1030
	4	53.64	915.7	1033
	5	65.82	917.0	1034
Uniform $q = \text{const}$	1	50.90	1596	1856
	2	51.59	1595	2098
	3	112.7	1597	2179
	4	113.0	1597	2181
	5	142.8	1597	2181
Point load P at the centre of the plate	1	22.92	3024	397.9
	2	23.04	3023	446.9
	3	33.28	3024	464.9
	4	33.33	3031	466.1
	5	38.12	3025	456.3

where $\tilde{w} = w_{\max} E_1 (10qh))^{-1}$ and $\tilde{\sigma} = \sigma_{\max} q^{-1}$

transverse shear. Moreover, the degrees of freedom of the nodal points of these elements are independent of the number of layers.

The approximations and degrees of freedom related to the different types of stress and strain states of the plate yield similar coefficients in the stiffness matrix and in the blocks comprising the stiffness matrix. A significant number of coefficients are the same as those of the classical theory, which simplifies the calculation of the stiffness matrix and allows the experience gained in using the finite element method in similar applications on the basis of classical theory to be extended to a non-classical approach based on the present higher-order theory.

The accuracy of the elements is illustrated by comparing the results with exact, analytical and finite element solutions of other authors. The results predicted by the approach presented here are found to be in excellent agreement with three-dimensional elasticity solutions.

The present investigation indicates that the finite elements proposed in this study are highly efficient and accurate, and may easily be incorporated into existing finite element packages.

Acknowledgement

The authors gratefully acknowledge the support of the Foundation for Research Development through a Core Programmes research grant.

References

[1] Dudchenko AA, Lur'e SA & Obraztsov IF. Anisotropic multilayer plates and shells. Summary of Science and Engineering. *Mechanica Deformiruemogo Tela*, 1983, **15**, pp.3–68 (in Russian).

[2] Noor AK & Burton WS. Assessment of computational models for multilayered composite shells. *Appl. Mech. Rev.*, 1990, **43**(4), pp.67–97.

[3] Reddy JN. A review of refined theories of laminated composite plates. *Shock Vib. Dig.*, 1990, **22**(7), pp.3–17.

[4] Reddy JN. On refined theories of composite laminates. *Meccanica*, 1990, **25**(4), pp.230–238.

[5] Librescu L & Reddy JN. A few remarks concerning several refined theories of anisotropic composite laminated plates. *Int. J. Eng. Sci.*, 1989, **27**(5), pp.515–527.

[6] Piskunov VG, Verijenko VE & Prisyazhnyuk VK. *Calculation of inhomogeneous shells and plates using finite element methods.* 1987, Veisha Shkola, Kiev, 200pp. (in Russian).

[7] Verijenko VE. Nonclassical theory of elasto-plastic strain of laminated transversely isotropic tapered shells. *Strengths of Materials*, 1987, **19**(4), pp.547–553.

[8] Verijenko VE, Adali S & Summers EB. Discrete-continuous scheme of FEM for analysing laminated composite shells and plates. *Proceedings of FEMSA92*, 1992, pp.589–600.

[9] Piskunov VG, Verijenko VE, Adali S & Summers EB. A higher order theory for the analysis of laminated plates and shells with shear and normal deformation. *Int. J. Eng. Sci.*, 1993, **31**(6), pp. 967–988.

[10] Piskunov VG & Verijenko VE. *Linear and nonlinear problems in the analysis of laminated structures.* 1986, Budivelnik, Kiev, 176pp. (in Russian).

[11] Verijenko VE & Prisyazhnyuk VK. Linear and non-linear models of contact interaction of laminated constructions with elastic basement. *International Congress IKM-X Weimar Germany*, 1984, **6**, pp.175–182.

[12] Clough RW & Penzien J. *Dynamics of structures.* 1975, McGraw-Hill, New York.

[13] Vlasov BF. On the bending of a rectangular thick plate. *Vest. Moscow University*, 1957, **2**, pp.22–34 (in Russian).

[14] Brukker, LE. Some variants of the equations for three-layered plates. *Journal of Analysis of Elements of Aviation Structures*, 1965, **3**, pp.74–99 (in Russian).

Appendix A

Elements of submatrix K_{11} for rectangular FE

$$k_{11} = k_{44} = k_{77} = k_{1010} = 4\frac{a}{b^3} + 4\frac{b}{a^3} + 2.8\frac{1}{ab} - 0.8\nu_{11}\frac{1}{ab}$$

$$k_{22} = k_{55} = k_{88} = k_{1111} = \frac{4}{3}\frac{a}{b} + \frac{4}{15}\frac{b}{a} - \frac{4}{15}\nu_{11}\frac{b}{a}$$

$$k_{33} = k_{66} = k_{99} = k_{1212} = \frac{4}{3}\frac{b}{a} + \frac{4}{15}\frac{a}{b} - \frac{4}{15}\nu_{11}\frac{a}{b}$$

$$k_{12} = k_{45} = -k_{78} = -k_{1011} = 2\frac{a}{b^2} + 0.2\frac{1}{a} + 0.8\nu_{11}\frac{1}{a}$$

$$k_{13} = -k_{46} = k_{79} = -k_{1012} = -2\frac{b}{a^2} - 0.2\frac{1}{b} - 0.8\nu_{11}\frac{1}{b}$$

$$k_{14} = k_{710} = 2\frac{a}{b^3} - 4\frac{b}{a^3} - 2.8\frac{1}{ab} + 0.8\nu_{11}\frac{1}{ab}$$

$$k_{15} = k_{24} = -k_{711} = -k_{810} = \frac{a}{b^2} - 0.2\frac{1}{a} - 0.8\nu_{11}\frac{1}{a}$$

$$k_{16} = -k_{34} = k_{712} = -k_{910} = -2\frac{b}{a^2} - 0.2\frac{1}{b} + 0.2\nu_{11}\frac{1}{b}$$

$$k_{17} = k_{410} = 2\frac{b}{a^3} - 4\frac{a}{b^3} - 2.8\frac{1}{ab} + 0.8\nu_{11}\frac{1}{ab}$$

$$k_{18} = -k_{27} = k_{411} = -k_{510} = 2\frac{a}{b^2} + 0.2\frac{1}{a} - 0.2\nu_{11}\frac{1}{a}$$

$$k_{19} = k_{37} = -k_{412} = -k_{610} = -\frac{b}{a^2} + 0.2\frac{1}{b}0.8\nu_{11}\frac{1}{b}$$

$$k_{110} = k_{47} = -2\frac{a}{b^3} - 2\frac{b}{a^3} + 2.8\frac{1}{ab} - 0.8\nu_{11}\frac{1}{ab}$$

$$k_{111} = -k_{210} = k_{48} = -k_{57} = \frac{a}{b^2} - 0.2\frac{1}{a} + 0.2\nu_{11}\frac{1}{a}$$

$$k_{112} = -k_{310} = -k_{49} = k_{67} = -\frac{b}{a^2} + 0.2\frac{1}{b} - 0.2\nu_{11}\frac{1}{b}$$

$$k_{23} = -k_{56} = -k_{89} = k_{1112} = -\nu_{11}$$

$$k_{25} = k_{811} = \tfrac{2}{3}\tfrac{a}{b} - \tfrac{4}{15}\tfrac{b}{a} + \tfrac{4}{15}\nu_{11}\tfrac{b}{a}$$

$$k_{26} = k_{35} = k_{812} = k_{911} = k_{29} = k_{38} = k_{512} = k_{611} = k_{212} = k_{311} = k_{59} = k_{68} = 0$$

$$k_{28} = k_{511} = \tfrac{2}{3}\tfrac{a}{b} - \tfrac{1}{15}\tfrac{b}{a} + \tfrac{1}{15}\nu_{11}\tfrac{b}{a}$$

$$k_{211} = k_{58} = \tfrac{1}{3}\tfrac{a}{b} + \tfrac{1}{15}\tfrac{b}{a} - \tfrac{1}{15}\nu_{11}\tfrac{b}{a}$$

$$k_{36} = k_{912} = \tfrac{2}{3}\tfrac{b}{a} - \tfrac{1}{15}\tfrac{a}{b} + \tfrac{1}{15}\nu_{11}\tfrac{a}{b}$$

$$k_{39} = k_{612} = \tfrac{2}{3}\tfrac{b}{a} - \tfrac{4}{15}\tfrac{a}{b} + \tfrac{4}{15}\nu_{11}\tfrac{a}{b}$$

$$k_{312} = k_{69} = \tfrac{1}{3}\tfrac{b}{a} + \tfrac{1}{15}\tfrac{a}{b} - \tfrac{1}{15}\nu_{11}\tfrac{a}{b}$$

Appendix B

Additional quantities for computation of the submatrix K_{22} for rectangular FE

$$\alpha_{11} = \alpha_{44} = \alpha_{77} = \alpha_{1010} = \tfrac{46}{105}\left(\tfrac{b}{a} + \tfrac{a}{b}\right)$$

$$\alpha_{12} = \alpha_{45} = -\alpha_{78} = -\alpha_{1011} = \tfrac{b}{30}\left(\tfrac{11}{7}\tfrac{b}{a} + \tfrac{a}{b}\right)$$

$$\alpha_{13} = -\alpha_{46} = \alpha_{79} = -\alpha_{1012} = \tfrac{a}{30}\left(\tfrac{11}{7}\tfrac{a}{b} + \tfrac{b}{a}\right)$$

$$\alpha_{14} = \alpha_{710} = \tfrac{1}{105}\left(17\tfrac{a}{b} - 46\tfrac{b}{a}\right)$$

$$\alpha_{15} = \alpha_{24} = -\alpha_{711} = -\alpha_{810} = \tfrac{b}{30}\left(2\tfrac{a}{b} - \tfrac{11}{7}\tfrac{b}{a}\right)$$

$$\alpha_{16} = -\alpha_{34} = \alpha_{712} = -\alpha_{910} = \tfrac{a}{30}\left(\tfrac{13}{14}\tfrac{a}{b} - \tfrac{b}{a}\right)$$

$$\alpha_{17} = \alpha_{410} = \tfrac{1}{105}\left(17\tfrac{b}{a} - 46\tfrac{a}{b}\right)$$

$$\alpha_{18} = -\alpha_{27} = \alpha_{411} - \alpha_{510} = \tfrac{b}{30}\left(\tfrac{a}{b} - \tfrac{13}{14}\tfrac{b}{a}\right)$$

$$\alpha_{19} = \alpha_{37} = -\alpha_{412} = -\alpha_{610} = \tfrac{a}{30}\left(\tfrac{11}{7}\tfrac{a}{b} - \tfrac{1}{2}\tfrac{b}{a}\right)$$

$$\alpha_{110} = \alpha_{47} - \tfrac{17}{105}\left(\tfrac{b}{a} + \tfrac{a}{b}\right)$$

$$\alpha_{111} = -\alpha_{210} = \alpha_{48} = -\alpha_{57} = \tfrac{b}{60}\left(\tfrac{13}{7}\tfrac{b}{a} + \tfrac{a}{b}\right)$$

$$\alpha_{112} = -\alpha_{310} = -\alpha_{49} = \alpha_{67} - \tfrac{a}{60}\left(\tfrac{13}{7}\tfrac{a}{b} + \tfrac{b}{a}\right)$$

$$\alpha_{22} = \alpha_{55} = \alpha_{88} = \alpha_{1111} = \tfrac{b^2}{15}\left(\tfrac{1}{7}\tfrac{b}{a} + \tfrac{2}{3}\tfrac{a}{b}\right)$$

$$\alpha_{25} = \alpha_{811} = \tfrac{b^2}{15}\left(\tfrac{1}{3}\tfrac{a}{b} - \tfrac{1}{7}\tfrac{b}{a}\right)$$

$$\alpha_{28} = \alpha_{511} = -\tfrac{b^2}{10}\left(\tfrac{1}{14}\tfrac{b}{a} + \tfrac{1}{9}\tfrac{a}{b}\right)$$

$$\alpha_{211} = \alpha_{58} = \tfrac{b^2}{20}\left(\tfrac{1}{7}\tfrac{b}{a} - \tfrac{1}{9}\tfrac{a}{b}\right)$$

$$\alpha_{33} = \alpha_{66} = \alpha_{99} = \alpha_{1212} = -\tfrac{a^2}{15}\left(\tfrac{1}{7}\tfrac{a}{b} + \tfrac{2}{3}\tfrac{b}{a}\right)$$

$$\alpha_{36} = \alpha_{912} = -\tfrac{a^2}{10}\left(\tfrac{1}{14}\tfrac{a}{b} + \tfrac{1}{9}\tfrac{b}{a}\right)$$

$$\alpha_{39} = \alpha_{612} = \tfrac{a^2}{15}\left(\tfrac{1}{3}\tfrac{b}{a} - \tfrac{1}{7}\tfrac{a}{b}\right)$$

$$\alpha_{312} = \alpha_{69} = \tfrac{a^2}{20}\left(\tfrac{1}{7}\tfrac{a}{b} - \tfrac{1}{9}\tfrac{b}{a}\right)$$

$$\alpha_{23} = \alpha_{56} = \alpha_{89} = \alpha_{1112} = \alpha_{26} = \alpha_{35} = \alpha_{812} = \alpha_{911} = \alpha_{29} = \alpha_{38} = \alpha_{512} = \alpha_{611} = \alpha_{212} = \alpha_{311} = \alpha_{59} = \alpha_{68} = 0$$